

Figure S1 (a) SEM images and (b) particle size distribution graphs of large cubes. Scale bars, 100 nm.

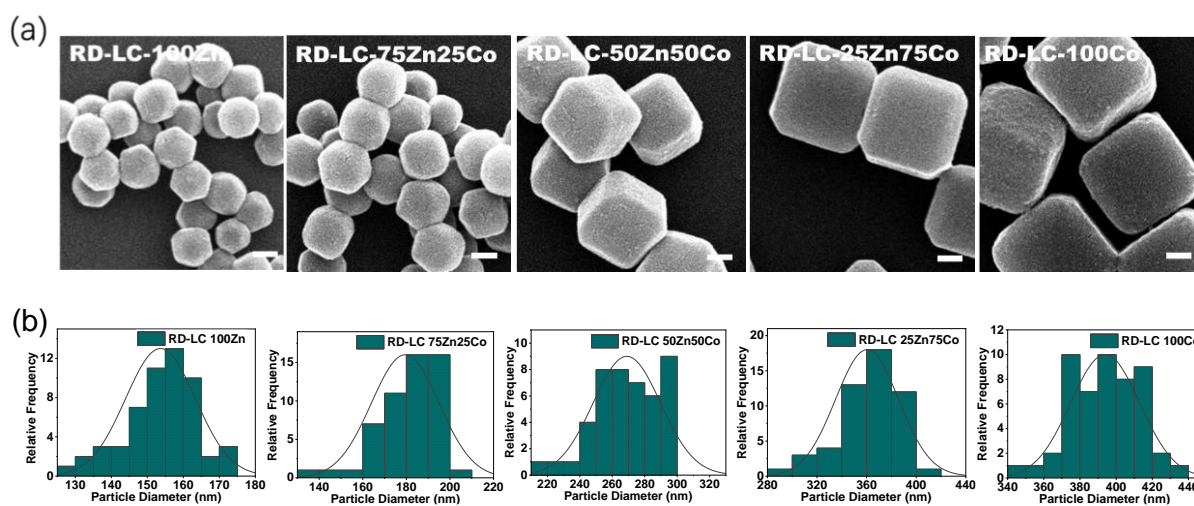


Figure S2 (a) SEM images and (b) particle size distribution graphs of rhombic dodecahedron - large cubes. Scale bars, 100 nm.

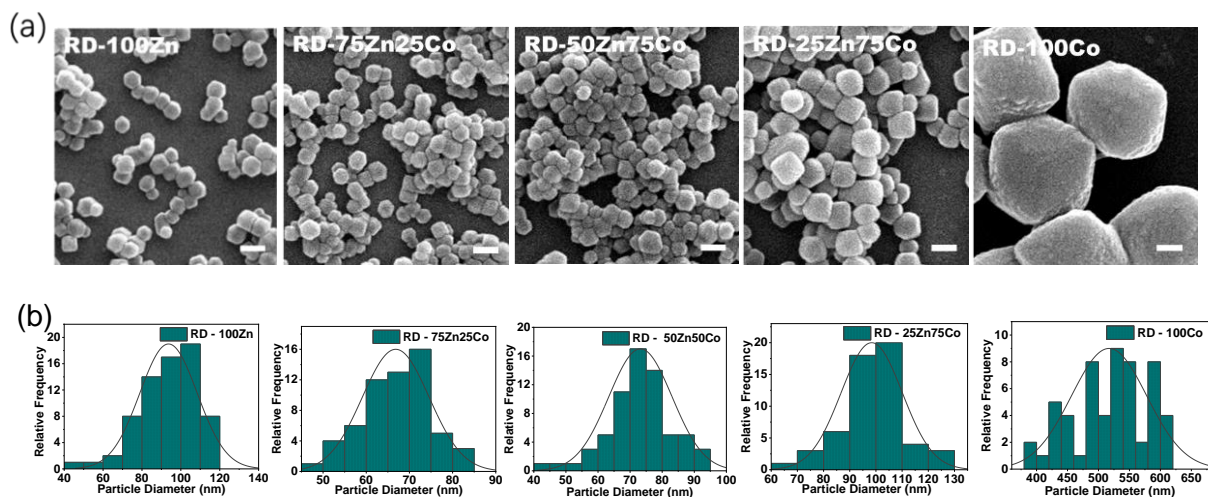


Figure S3 (a) SEM and (b) particle size distribution of rhombic dodecahedron. Scale bars, 100 nm.

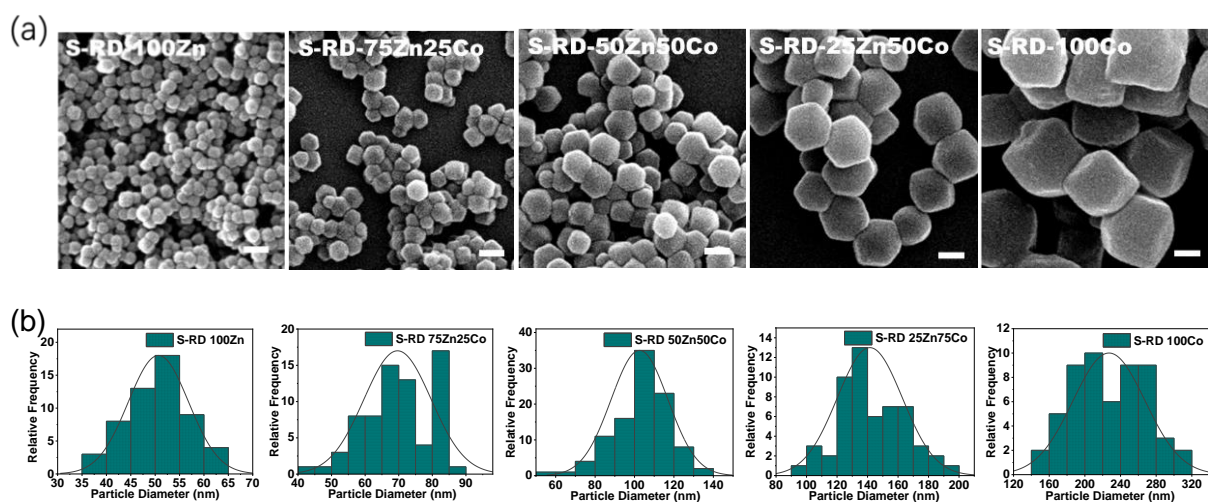


Figure S4 (a) SEM images and (b) particle size distribution graphs of spherical - rhombic dodecahedron. Scale bars, 100 nm.

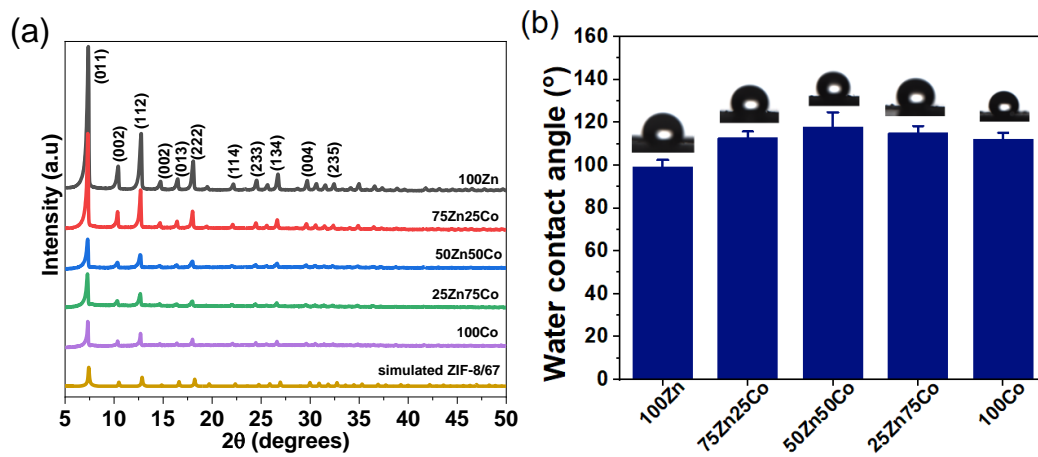


Figure S5 (a) XRD patterns and (b) Water contact angles of large cubes.

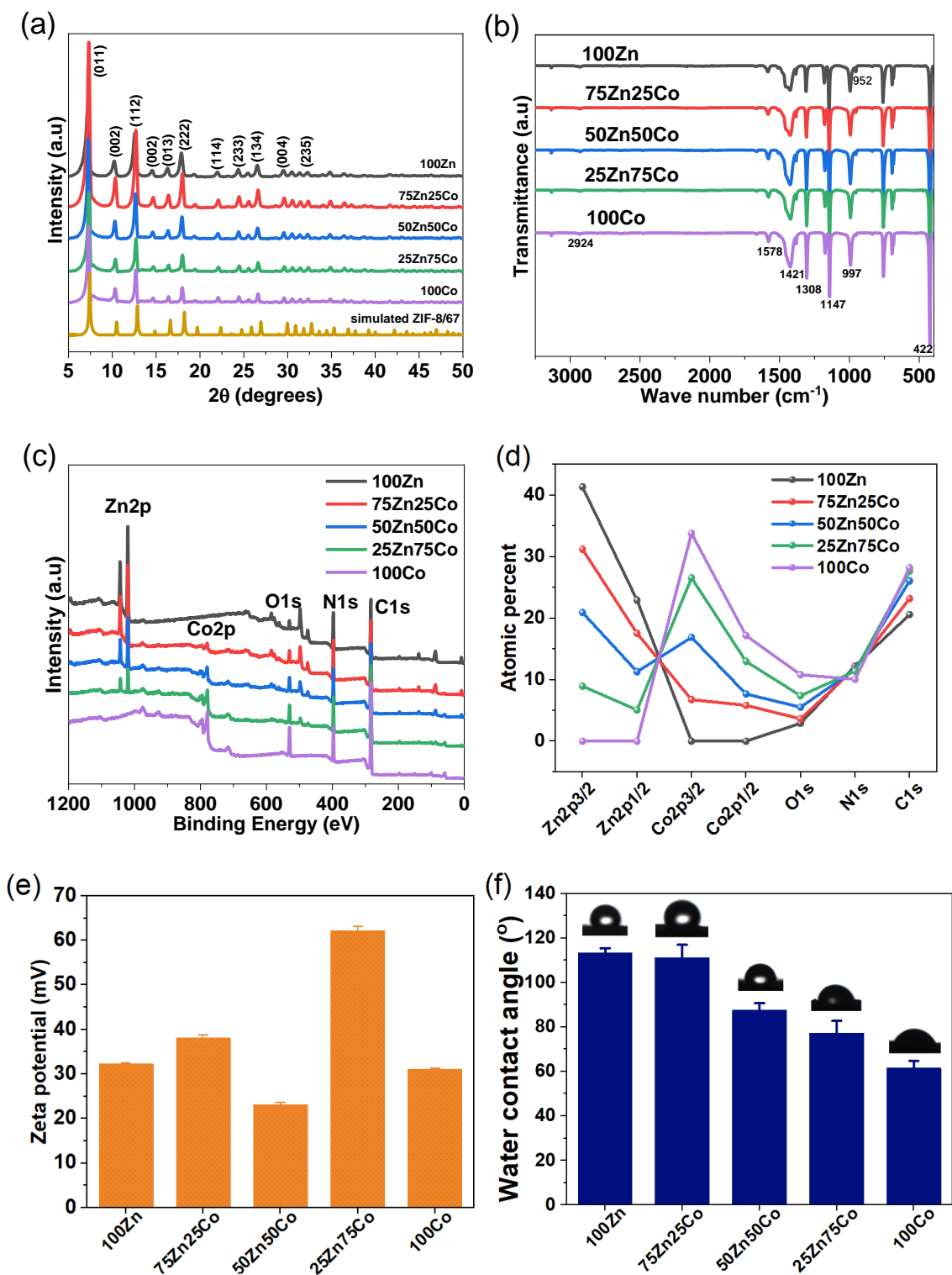


Figure S6 (a) XRD patterns, (b) FT-IR absorption spectra, (c) XPS survey spectra, (d) Atomic percent of various orbital levels extracted from XPS spectra, (e) Zeta potentials, and (f) Water contact angles of spherical - rhombic dodecahedron group.

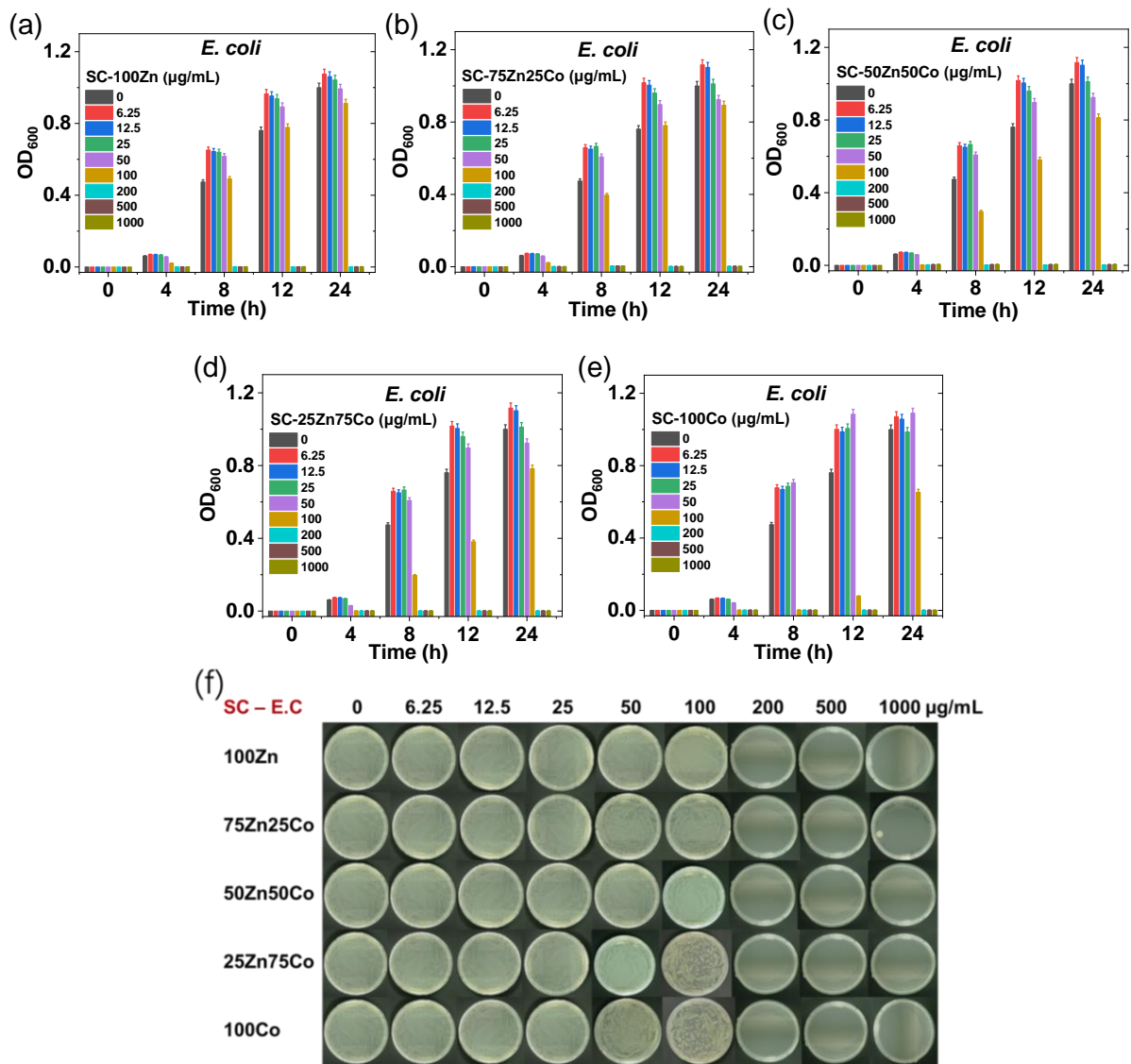


Figure S7 Bacterial cell viability of *E. coli* measured at various time intervals after being exposed to different concentrations of (a) SC-100Zn, (b) SC-75Zn25Co, (c) SC-50Zn50Co, (d) SC-25Zn75Co, and (e) SC-100Co. (f) Corresponding photographs of bacterial colony with different treatments in agar plates. Data are provided as the mean \pm SD, n = 3.

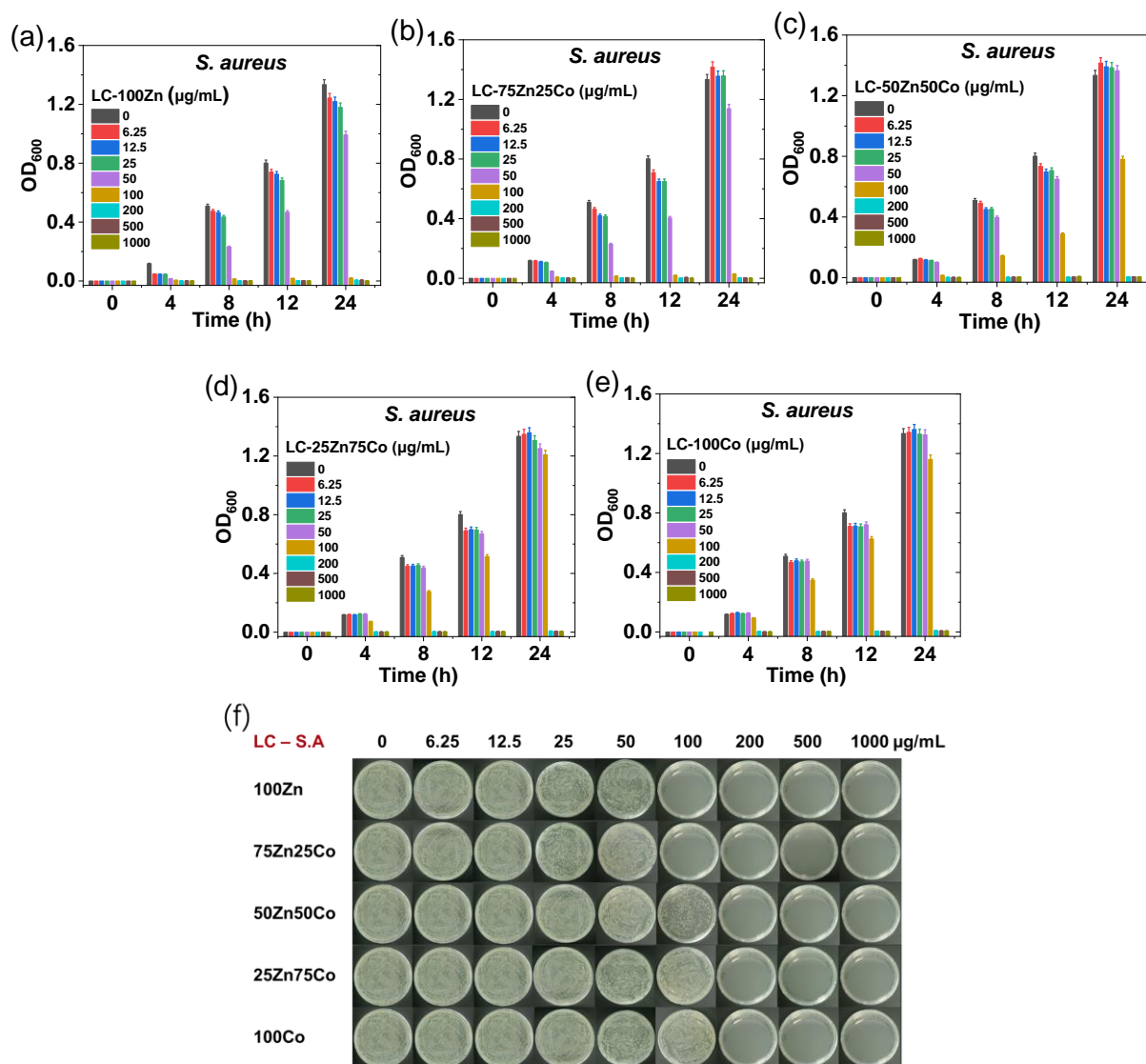


Figure S8 Bacterial cell viability of *S. aureus* measured at various time intervals after being exposed to different concentrations of (a) LC-100Zn, (b) LC-75Zn25Co, (c) LC-50Zn50Co, (d) LC-25Zn75Co, and (e) LC-100Co. (f) Corresponding photographs of bacterial colony with different treatments in agar plates. Data are provided as the mean \pm SD, n = 3.

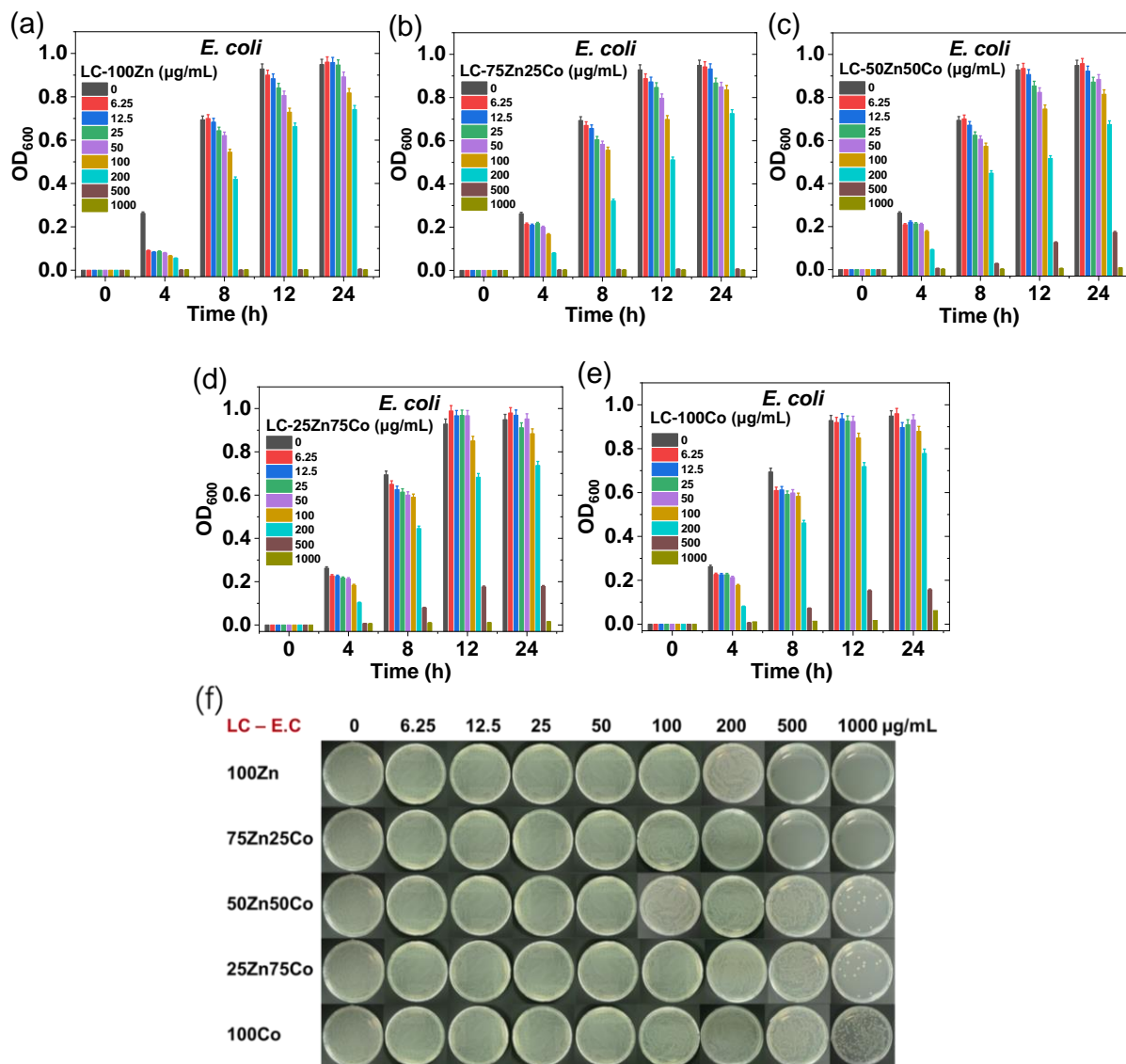


Figure S9 Bacterial cell viability of *E. coli* measured at various time intervals after being exposed to different concentrations of (a) LC-100Zn, (b) LC-75Zn25Co, (c) LC-50Zn50Co, (d) LC-25Zn75Co, and (e) LC-100Co. (f) Corresponding photographs of bacterial colony with different treatments in agar plates. Data are provided as the mean \pm SD, $n = 3$.

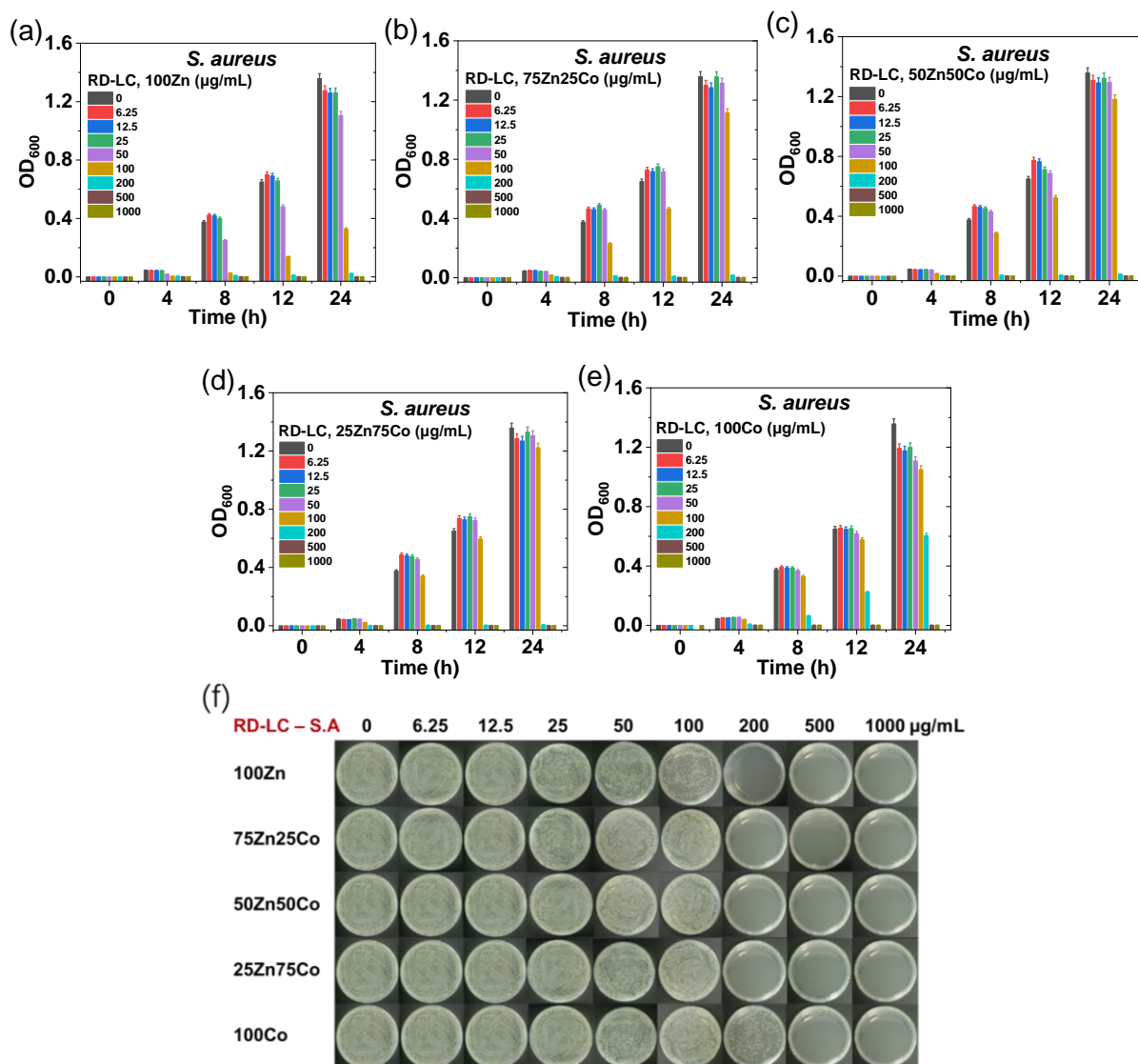


Figure S10 Bacterial cell viability of *S. aureus* measured at various time intervals after being exposed to different concentrations of (a) RD-LC-100Zn, (b) RD-LC-75Zn25Co, (c) RD-LC-50Zn50Co, (d) RD-LC-25Zn75Co, and (e) RD-LC-100Co. (f) Corresponding photographs of bacterial colony with different treatments in agar plates. Data are provided as the mean \pm SD, n = 3.

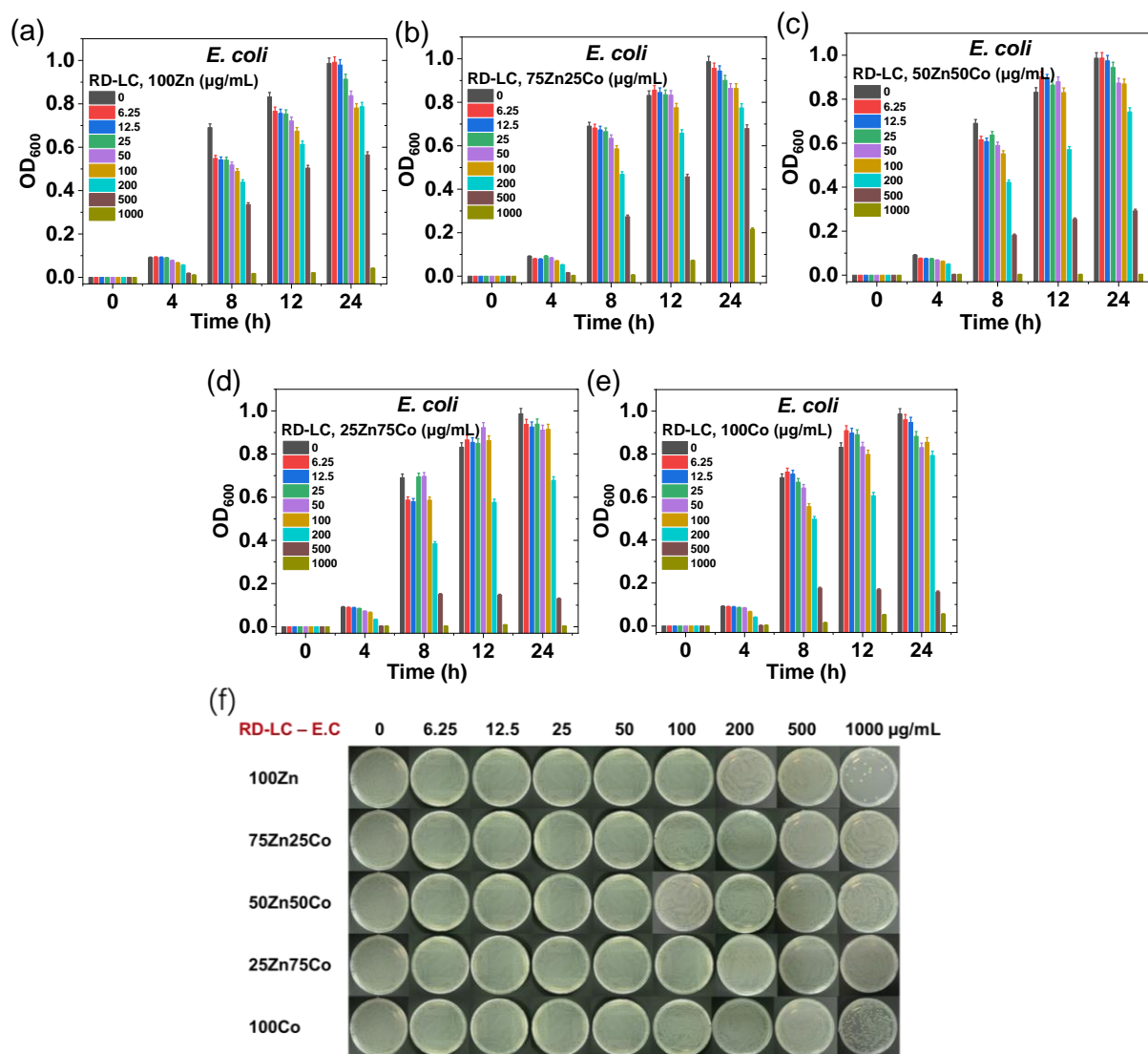


Figure S11 Bacterial cell viability of *E. coli* measured at various time intervals after being exposed to different concentrations of (a) RD-LC-100Zn, (b) RD-LC-75Zn25Co, (c) RD-LC-50Zn50Co, (d) RD-LC-25Zn75Co, and (e) RD-LC-100Co. (f) Corresponding photographs of bacterial colony with different treatments in agar plates. Data are provided as the mean \pm SD, $n = 3$.

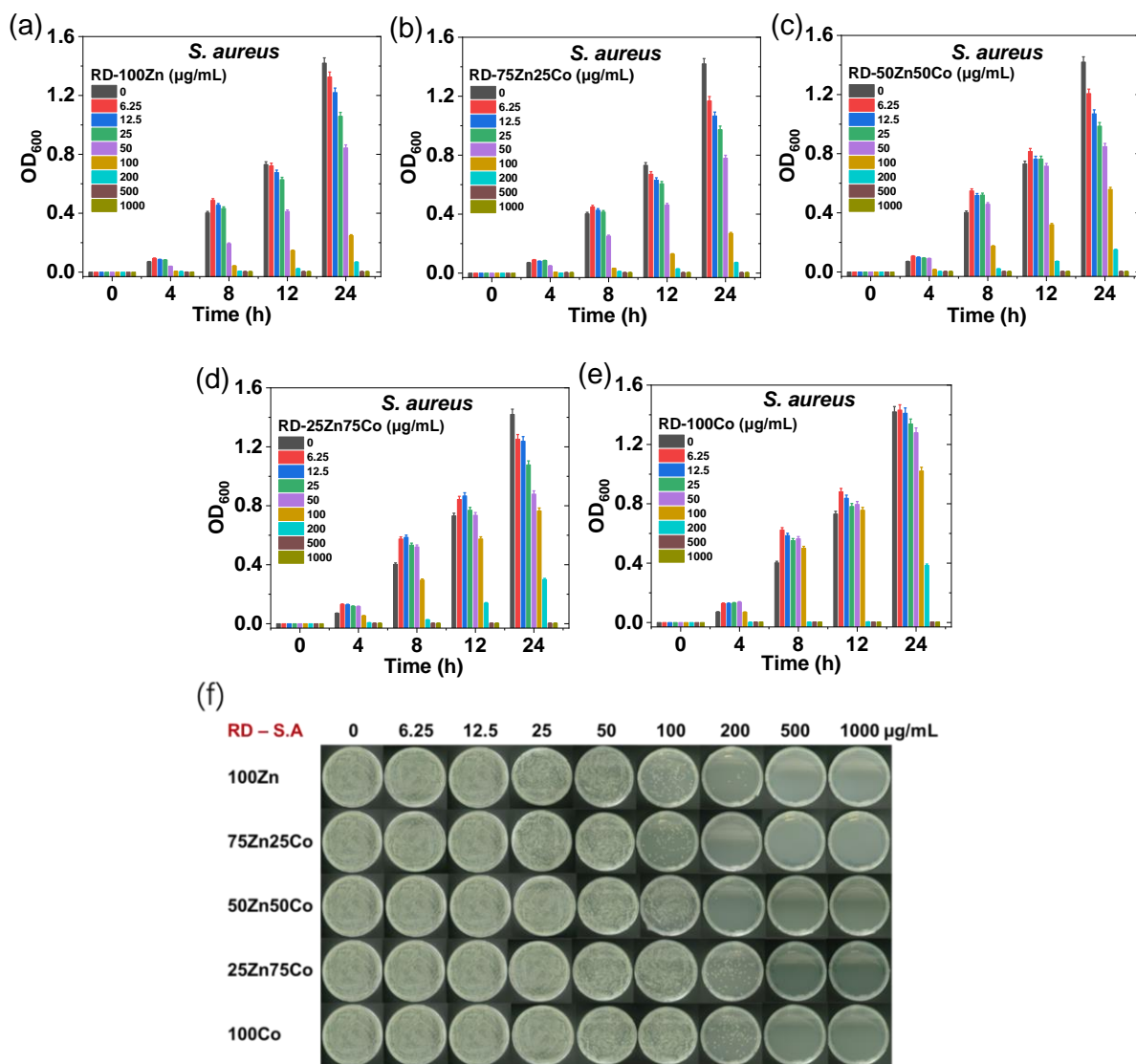


Figure S12 Bacterial cell viability of *S. aureus* measured at various time intervals after being exposed to different concentrations of (a) RD-100Zn, (b) RD-75Zn25Co, (c) RD-50Zn50Co, (d) RD-25Zn75Co, and (e) RD-100Co. (f) Corresponding photographs of bacterial colony with different treatments in agar plates. Data are provided as the mean \pm SD, $n = 3$.

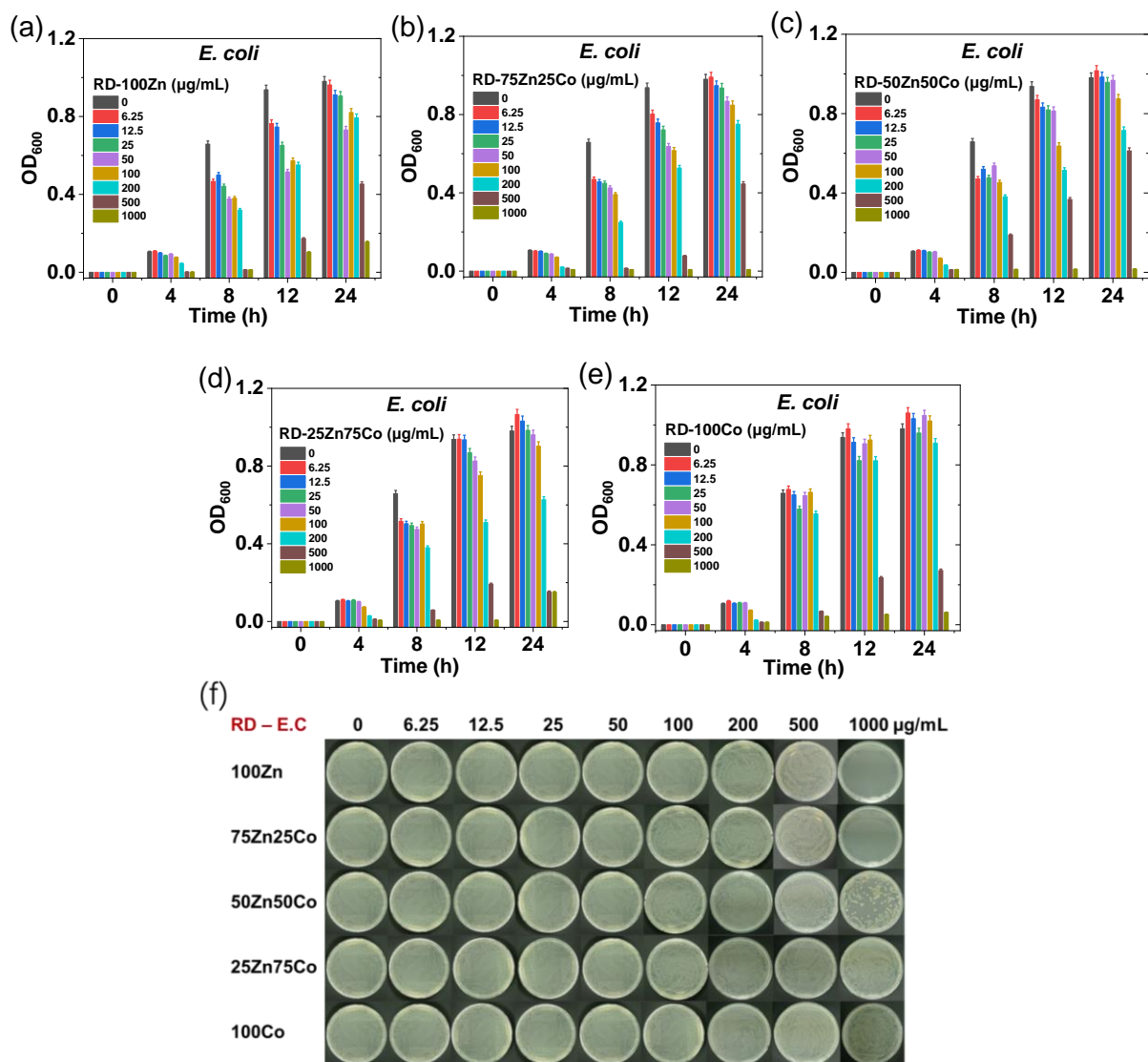


Figure S13 Bacterial cell viability of *E. coli* measured at various time intervals after being exposed to different concentrations of (a) RD-100Zn, (b) RD-75Zn25Co, (c) RD-50Zn50Co, (d) RD-25Zn75Co, and (e) RD-100Co. (f) Corresponding photographs of bacterial colony with different treatments in agar plates. Data are provided as the mean \pm SD, n = 3.

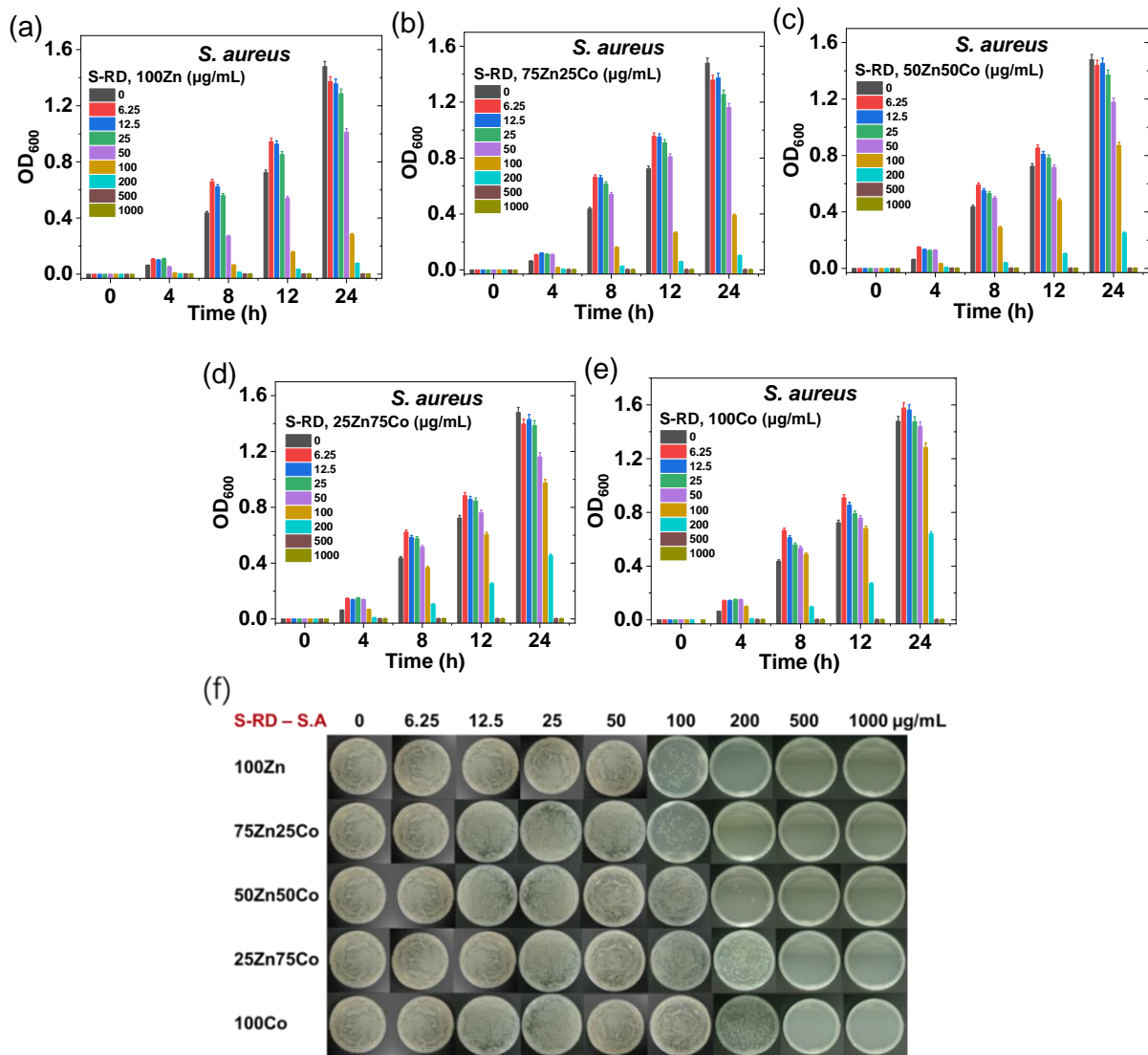


Figure S14 Bacterial cell viability of *S. aureus* measured at various time intervals after being exposed to different concentrations of (a) S-RD-100Zn, (b) S-RD-75Zn25Co, (c) S-RD-50Zn50Co, (d) S-RD-25Zn75Co, and (e) S-RD-100Co. (f) Corresponding photographs of bacterial colony with different treatments in agar plates. Data are provided as the mean \pm SD, n = 3.

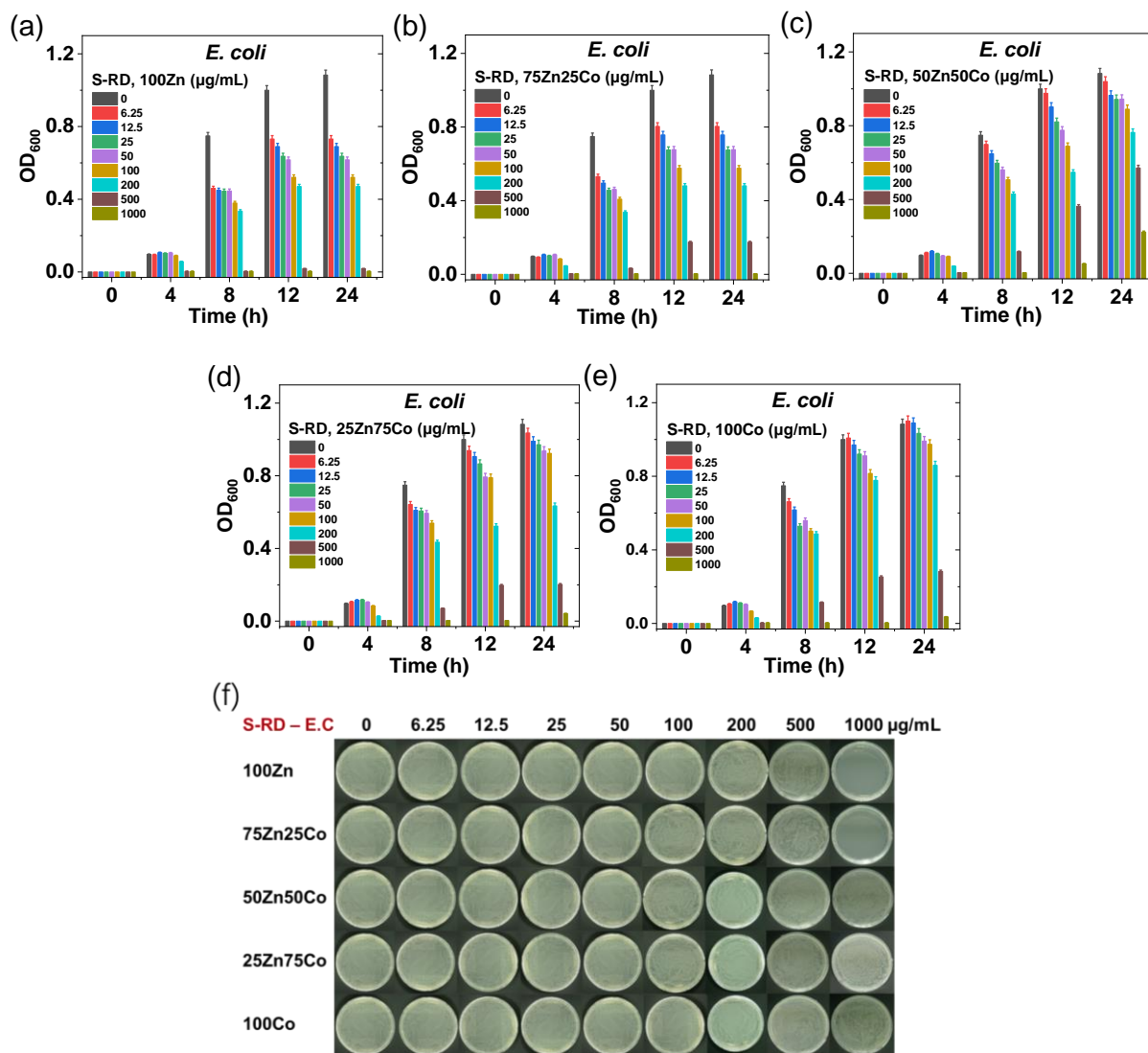


Figure S15 Bacterial cell viability of *E. coli* measured at various time intervals after being exposed to different concentrations of (a) S-RD-100Zn, (b) S-RD-75Zn25Co, (c) S-RD-50Zn50Co, (d) S-RD-25Zn75Co, and (e) S-RD-100Co. (f) Corresponding photographs of bacterial colony with different treatments in agar plates. Data are provided as the mean \pm SD, n = 3.

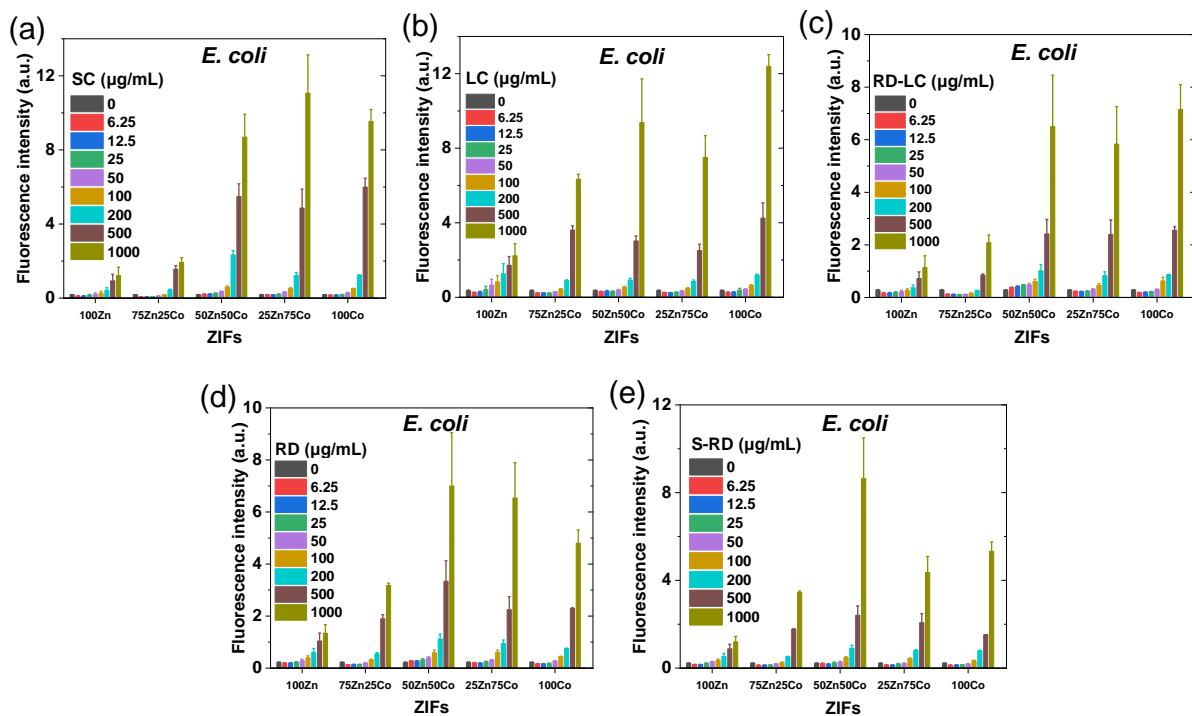


Figure S16 ROS generation in *E. coli* after exposure to various concentrations of ZIFs using DCFH-DA. Data are provided as the mean \pm SD, n = 3.

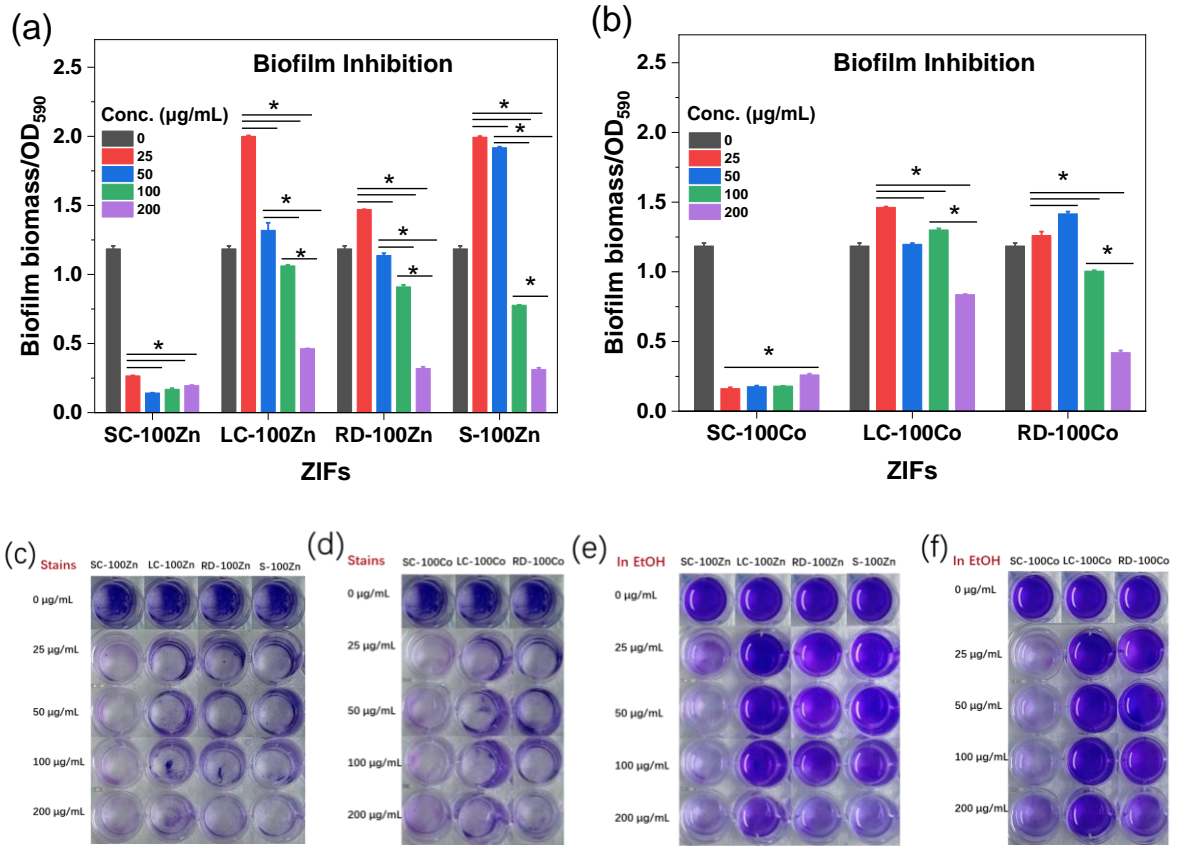


Figure S17 The effect of ZIFs on inhibiting biofilms. Biofilm biomass treated with different concentrations of (a) 100Zn and (b) 100Co. Pictures of crystal violet-stained biofilms treated with (c) 100Zn and (d) 100Co. Pictures of crystal violet-stained biofilms dissolved in ethanol (e) 100Zn and (f) 100Co. Data are provided as the mean \pm SD, n = 3. *P < 0.05.

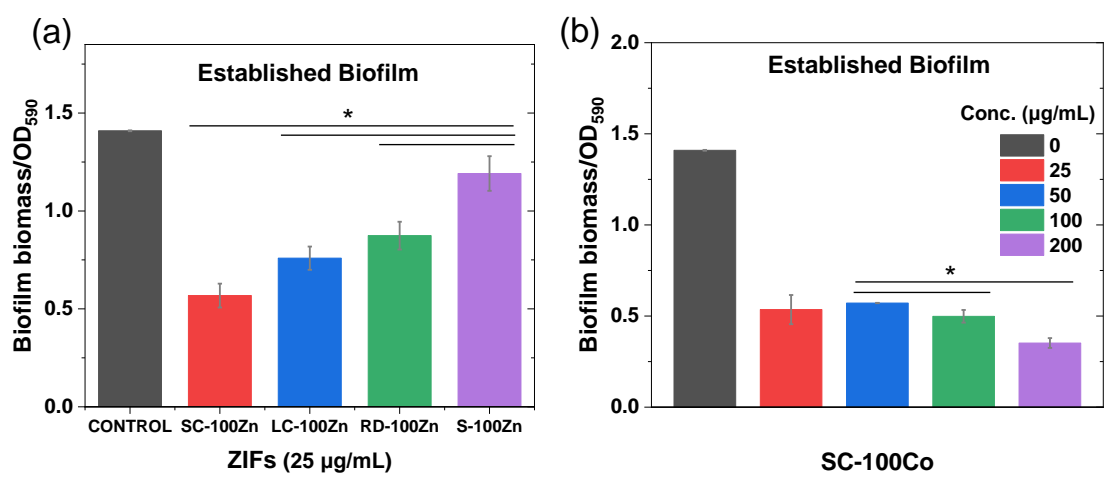


Figure S18 The effect of ZIFs on eliminating the established biofilms. Biofilm biomass treated with different concentrations of ZIFs: (a) 100Zn group (b) SC-100Co. Data are provided as the mean \pm SD, n = 3. *P < 0.05.

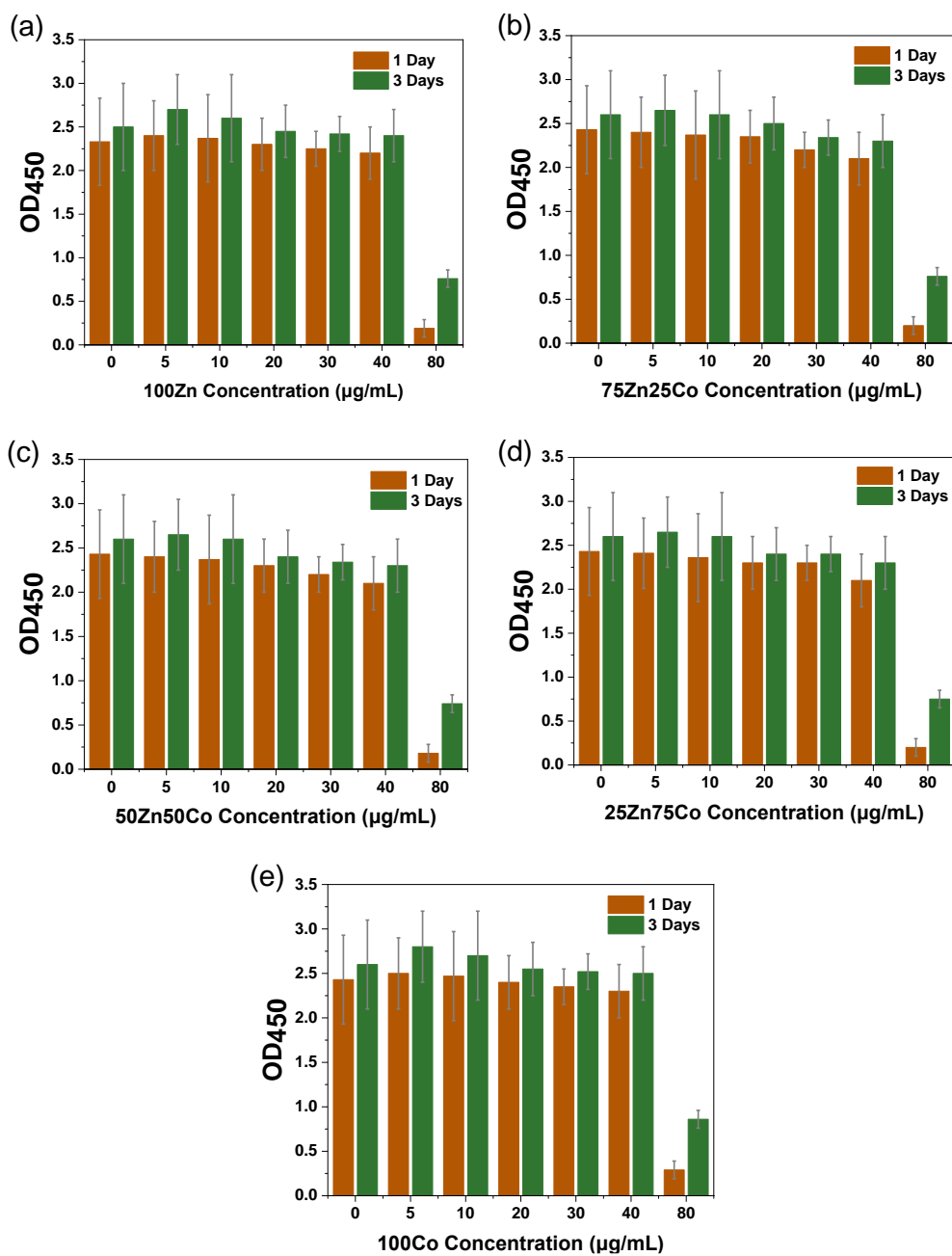


Figure S19 Cytotoxicity evaluation of (a) 100Zn, (b) 75Zn25Co, (c) 50Zn50Co, (d) 25Zn75Co, and (e) 100Co ZIF particles